Theor Chem Acc (1997) 97:59–66

Theoretical
Chemistry Accounts

The inner-hydrogen migration in free base porphyrin

Jon Baker, Pawel M. Kozlowski*, Andrzej A. Jarzecki, Peter Pulay**

Department of Chemistry and Biochemistry, University of Arkansas, Fayetteville, AR 72701, USA

Received: 27 January 1997 / Accepted: 8 April 1997

Abstract. We present the results of a comprehensive study on the inner-hydrogen migration in free base porphyrin, using density functional theory with the hybrid B3-LYP exchange-correlation functional, and both the 6-31G(*d*) and a triple-zeta double-polarization (TZ2P) basis set. The latter computations, involving 726 contracted functions, are the largest calculations on this system to date. Full geometry optimization was carried out for the *cis* and *trans* minima, the transition state for *trans-cis* isomerization, and the symmetric stationary point for the synchronous *trans-trans* isomerization. All stationary points were characterized by vibrational analysis. Our results strongly support the conclusion, reached by earlier workers, that *trans-trans* hydrogen transfer occurs in a two-step process via a *cis* intermediate. With the TZ2P basis and including zero-point effects for the -h_2 isotopomer, the *trans-cis* barrier height is 13.1 kcal/mol, the *cis-trans* energy difference is 8.1 kcal/mol and the reverse *cis-trans* barrier height is 5.0 kcal/mol. The *trans-cis* barrier height agrees well with the value of Braun et al. (J Am Chem Soc (1996) 118: 7231) obtained from NMR line shapes and a modified Bell tunneling model, but our *cis-trans* energy difference is higher, and the reverse barrier is lower, than the values of Braun et al. Tunneling precludes the existence of -h_2 *cis*-porphyrin as an observable species, but the -d_2 and, especially, -t_2 isotopomers might be observable at low temperatures if the reverse barrier is higher than our calculated value. We predict the theoretical vibrational spectrum of *cis*-porphyrin and suggest that IR active modes at 566 cm^{-1} and 2333 cm^{-1} in the -d_2 isotopomer may be used to detect the presence of the *cis* intermediate.

Key words: DFT – Dynamics – Barrier height – Isomerization

*Present address: Department of Chemistry, Princeton University, Princeton, NJ 08544, USA
**Present address: Department of Chemistry, Indiana University, Bloomington, IN 47405, USA
Correspondence to: J. Baker or P. Pulay

1 Introduction

Porphyrins and metalloporphyrins play a central role in photosynthesis, in biological redox reactions and in oxygen transport, and have been intensively studied for many years [1, 2]. Interestingly, the symmetry of free base porphyrin was not definitely established until very recently. The X-ray diffraction analyses of Webb and Fleischer [3] and Chen and Tulinsky [4] indicate that, to a first approximation, the porphyrin molecule is planar, possessing good C_{2h} symmetry with respect to bond distances and angles and approximate D_{2h} symmetry overall. However, the X-ray structure is not fully conclusive for the geometry of the free molecule. Moreover, the X-ray results of Ref. [4], which show localized inner hydrogens, are apparently in conflict with solid-state NMR results [5], which indicate fast tautomerization at room temperature. Experimental IR spectra, for example the excellent matrix spectra of Radziszewski et al. [6], have been assigned on the basis of D_{2h} symmetry, but offer no conclusive proof by themselves.

Early calculations on porphyrin were restricted to closed-shell SCF (RHF) computations [7]. At this level of theory, both semiempirical [8, 9] and ab initio methods [10, 11] predict a symmetry-broken C_{2v} structure. For a while it was not completely clear whether symmetry breaking was an artifact of Hartree-Fock theory or a real phenomenon, although most researchers believed that the symmetry of the ground state was D_{2h}. Almlöf and coworkers [11] showed that inclusion of electron correlation restores the higher symmetry. Their fully optimized MP2 and local density functional theory (DFT) calculations both predict a D_{2h} ground state (Fig. 1a). This prediction has been verified using multireference wavefunctions by Merchan et al. [12] and by Kozlowski et al. [13] using non-local hybrid density functional calculations. The most conclusive evidence for D_{2h} symmetry is the accurate reproduction of ground-state vibrational spectra (in particular the high-resolution matrix IR spectrum [6]), including the sym-

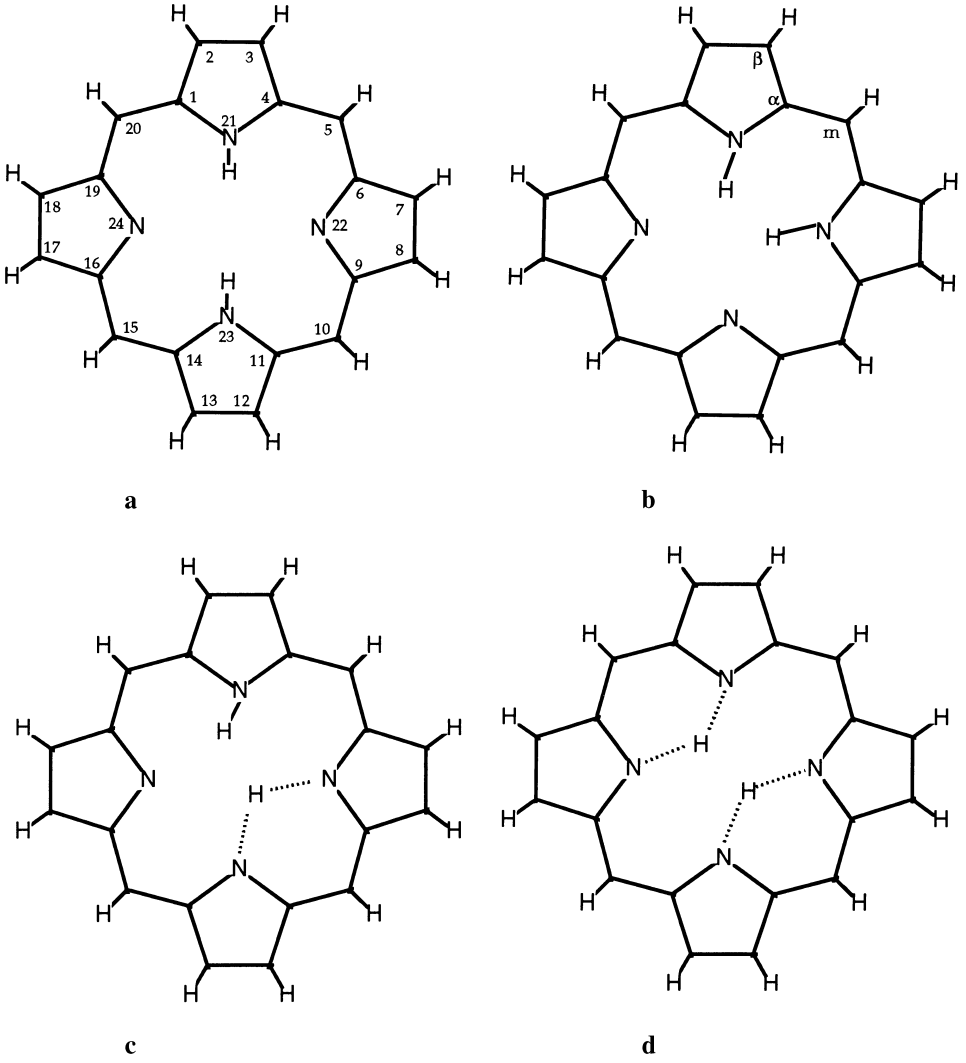

Fig. 1a–d. Structures of the four stationary points on the porphyrin PES relevant to the inner-hydrogen migration showing the atom labelling corresponding to the geometrical parameters reported in Table 1: **a** *trans*-porphyrin (D_{2h}); **b** *cis*-porphyrin (C_{2v}); **c** *trans-cis* transition state (TS; c_s); **d** second-order saddle point (SS; D_{2h})

metry-breaking B_{3u} modes, by DFT force fields derived at the optimized D_{2h} structure [14, 15].

A major topic of interest in free base porphyrin is the tautomerism of the two inner hydrogen atoms. This has been the subject of a number of experimental NMR studies [5, 16–19]. At low temperatures (below -30^{o} C), ^{13}C, ^{1}H and ^{15}N NMR spectra show that the two kinds of pyrrole ring in the porphyrin molecule are inequivalent. As the temperature is raised, the signals broaden and coalesce into just one sharp peak. This is consistent with hydrogen transfer which is fast on the NMR timescale at room temperature but is frozen at low temperatures.

It is now generally accepted that the hydrogen transfer occurs via a two-step mechanism involving a metastable *cis* intermediate (C_{2v} symmetry; Fig. 1b) [18] rather than by a synchronous one-step procedure that had been proposed by some authors [20]. The observed rate is likely to be affected by tunneling, although by how much is not clear. Current experimental estimates put the *trans* $\longrightarrow$ *cis* activation energy at between 12–16 kcal/mol and the *cis-trans* energy difference at around 5 kcal/mol [21].

Theoretically, although *trans* porphyrin has been investigated with full geometry optimization at correlated levels (both MP2 [11] and B3-LYP including a full vibrational analysis [13–15]), the best calculations we are aware of on the *cis* isomer, those of Ghosh and Almlöf [22], involve only MP2 single-point energies at an LDA optimized geometry, and the *trans-cis* transition state has not been characterized at all at correlated levels apart from a *partial* optimization at the MP2 level by Reimers et al. [23]. All these calculations used basis sets of roughly split-valence + polarization quality.

The aim of this work is to provide a comprehensive picture of the inner-hydrogen migration in free base porphyrin, incorporating the effects of electron correlation, with full geometry optimization and characterization of all stationary points on the reaction path. We also predict the IR spectrum of the *cis* isomer, in the hope that it may guide experimentalists in the detection of *cis*-porphyrin in the presence of the more stable *trans* ground state. The calculations reported in this work are, we believe, the most accurate thus far on this important system. Our predictions differ in some important points from the latest theoretical results [23].

2 Computational details

The basic level of theory used throughout our study was DFT with the hybrid B3-LYP [24, 25] exchange-correlation functional as implemented in the Gaussian suite of programs [26], using the 6–31G(d) basis set (B3-LYP/6-31G(d)). DFT is currently the most cost-effective method available for including electron correlation, and hybrid functionals are currently the most accurate density functionals [27]. It appears that hybrid DFT approaches are very successful for transition states [28], especially those like the present one which do not have a strong biradical character [29].

All stationary points located on the B3-LYP/6-31G(d) porphyrin ground state potential energy surface were fully characterized by vibrational analysis using analytical second derivatives. Following our preliminary analysis using the 6-31G(d) basis, we reoptimized all structures using a much larger TZ2P basis [30] comprising a total of 726 contracted Gaussians, to give our final values for the *trans-cis* energy difference and barrier height. This basis set has been used in several recent DFT studies and is known to perform well [31, 32]. We used five spherical harmonic components as opposed to six Cartesian in the d-polarization functions for both bases. We have also carried out single-point MP2 calculations with the 6-31G(d) basis at the B3-LYP stationary points. The bulk of our calculations were done on local IBM 390 workstations using GAUSSIAN 94 [26].

3 Results

The four stationary points on the porphyrin potential energy surface (PES) relevant to the inner-hydrogen migration are the global *trans* minimum (D_{2h}; Fig. 1a), the metastable *cis* minimum (C_{2v}; Fig. 1b), the *trans-cis* transition state (C_s; Fig. 1c) and the SS structure (D_{2h}; Fig. 1d) which is a second-order saddle point or hilltop. The latter would be the most likely transition state if the *trans-trans* inner-hydrogen migration involved a synchronous double proton transfer.

These four structures were all located and characterized at the B3-LYP/6-31G(d) level of theory. The TS structure is a true transition state; the calculated imaginary frequency for the reaction coordinate, $1583i$ cm^{-1}, falls in the range obtained from modeling the experimental tautomerization rates by Butenhoff and Moore [21]. In their more probable model, using the lower value for the pre-exponential factor (5×10^{12}), they obtain imaginary frequencies between $1425i$ and $1853i$ cm^{-1}. The SS structure has two imaginary frequencies ($1560i$ cm^{-1} and $1465i$ cm^{-1}; unscaled), whose normal modes have B_{3g} and B_{2u} symmetry, respectively. Following the B_{3g} mode downhill lowers the symmetry to C_{2h} and leads to the *trans* minimum; similarly, following the B_{2u} mode downhill lowers the symmetry to C_{2v} and leads to the *cis* minimum. Distorting the original SS geometry along either mode and reoptimizing within C_{2h} or C_{2v} symmetry, searching now for a transition state, leads back to the SS structure. Having carried out these additional calculations, we are confident that we have located the only stationary points on the porphyrin PES relevant to the hydrogen migration. A schematic of the PES is given in Fig. 2. Note that this differs qualitatively from the PES in Fig. 2 of Ref. [23]. After locating these structures with the 6–31G(d) basis, we reoptimized all four species with the larger TZ2P basis to give our final geometries and energetics.

The most important geometrical parameters for all four species are listed in Table 1. For the *trans* ground state we also give the X-ray bond lengths of Webb and Fleischer [3] and the crystal geometry of Chen and Tulinsky [4]. Averaged bond lengths of the latter under full D_{2h} symmetry are given in parentheses. In discussing the average structures, we use the notation C_α, C'_α, where the primed atoms belong to the protonated rings (Fig. 1b).

Comparing the calculated B3-LYP geometries for *trans*-porphyrin, there is, as expected, a consistent shortening of all bond lengths by about 0.005 Å on going from the 6–31G(d) to the larger TZ2P basis. This is observed for all four structures. Bond angles are essentially unchanged. The distance contraction brings the calculated C—C bond lengths, which were already good with the 6–31G(d) basis, into even better agreement with the averaged experimental values. The average calculated heavy atom (C—C and C—N) bond distance is 1.394 Å, the same as in the X-ray structure of Ref. [4] and only 0.004 Å longer than the average of Ref. [3]. However, the deviations from this average differ considerably between the calculated geometry and the averaged X-ray structure of Ref. [4]. The discrepancy is particularly large for the C_α—C_m and C_α—N distances, almost 0.02 Å in both cases, with opposite sign. For the other C—C bonds, the discrepancy is 0.006 Å or less. The calculated C—N distances agree significantly better with the older X-ray diffraction results of Webb and

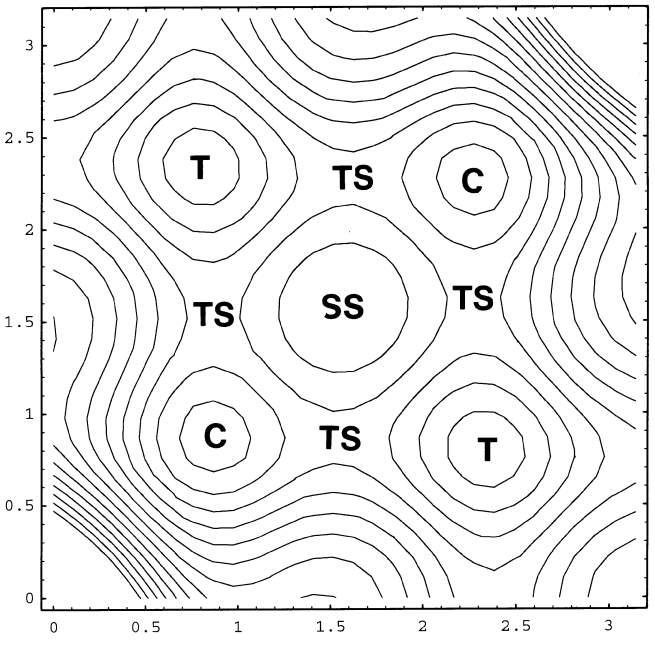

Fig. 2. Schematic of the porphyrin PES showing the *trans* minimum (*T*), the metastable *cis* minimum (*C*), the *trans-cis* transition state (*TS*) and the second-order saddle point (*SS*).

Table 1. Main Ring parameters (bond lengths in Å; bond angles in degrees) for the stationary points on the porphyrin PES. (Experimental values for *trans*-porphyrin from Refs. [3, 4] values in parentheses are averaged from Ref. [4] assuming exact D_{2h} symmetry)[a]

Parameter	*trans*					*cis*		TS		SS	
	6-31G(*d*)	TZ2P	XR[3]	XR[4]	Aver.	6-319G(*d*)	TZ2P	6-319G(*d*)	TZ2P	6-319G(*d*)	TZ2P
$rN_{21}H_1$	1.015	1.010		0.86[b]		1.027	1.022	1.026	1.021	1.298	1.296
$rN_{22}H_2$	2.310	2.308				1.027	1.022	1.289	1.286	1.298	1.296
$rN_{23}H_2$	1.015	1.010		0.86[b]		1.940	1.941	1.336	1.335	1.298	1.296
$\angle C_4N_{21}H_1$	124.6	124.6		120.3	(124.6)	131.9	132.0	130.4	130.4	145.8	146.0
$\angle C_6N_{22}H_2$	155.8	155.6				131.9	132.0	147.2	147.4	145.8	146.0
$\angle C_{11}N_{23}H_2$	124.6	124.6		129.0		101.9	101.7	105.9	105.6	106.8	106.5
rC_1C_2	1.435	1.431	1.441	1.437	(1.431)	1.432	1.427	1.433	1.428	1.440	1.435
rC_2C_3	1.372	1.367	1.340	1.359	(1.365)	1.372	1.367	1.373	1.368	1.363	1.358
rC_3C_4	1.435	1.431	1.436	1.425		1.438	1.433	1.438	1.433	1.452	1.447
rC_4C_5	1.394	1.389	1.386	1.384	(1.387)	1.397	1.391	1.394	1.388	1.397	1.391
rC_5C_6	1.400	1.395	1.382	1.373	(1.376)	1.397	1.391	1.399	1.393	1.397	1.391
rC_6C_7	1.461	1.456	1.447	1.449	(1.452)	1.438	1.433	1.450	1.445	1.452	1.447
rC_7C_8	1.357	1.351	1.344	1.346	(1.345)	1.372	1.367	1.362	1.356	1.363	1.358
rC_8C_9	1.461	1.456	1.440	1.456		1.432	1.427	1.437	1.433	1.440	1.435
rC_9C_{10}	1.400	1.395	1.389	1.375		1.395	1.389	1.394	1.389	1.396	1.391
$rC_{10}C_{11}$	1.394	1.389	1.390	1.398		1.403	1.397	1.397	1.391	1.396	1.391
$rC_{11}C_{12}$	1.435	1.431	1.439	1.434		1.459	1.454	1.440	1.436	1.440	1.435
$rC_{12}C_{13}$	1.372	1.367	1.341	1.371		1.358	1.352	1.362	1.356	1.363	1.358
$rC_{13}C_{14}$	1.435	1.431	1.438	1.427		1.465	1.460	1.453	1.449	1.452	1.447
$rC_{14}C_{15}$	1.394	1.389	1.383	1.378		1.401	1.396	1.399	1.393	1.397	1.391
$rC_{15}C_{16}$	1.400	1.395	1.385	1.375		1.401	1.396	1.398	1.393	1.397	1.391
$rC_{16}C_{17}$	1.461	1.456	1.449	1.439		1.465	1.460	1.464	1.459	1.452	1.447
$rC_{17}C_{18}$	1.357	1.351	1.341	1.344		1.358	1.352	1.359	1.353	1.363	1.358
$rC_{18}C_{19}$	1.461	1.456	1.448	1.465		1.459	1.454	1.458	1.454	1.440	1.435
$rC_{19}C_{20}$	1.400	1.395	1.385	1.382		1.403	1.397	1.401	1.395	1.396	1.391
$rC_{20}C_1$	1.394	1.389	1.390	1.388		1.395	1.389	1.396	1.390	1.396	1.391
rC_1N_{21}	1.373	1.368	1.359	1.377	(1.380)	1.379	1.374	1.375	1.370	1.375	1.370
$rN_{21}C_4$	1.373	1.368	1.368	1.379		1.374	1.370	1.367	1.362	1.367	1.363
rC_6N_{22}	1.363	1.358	1.373	1.363	(1.377)	1.374	1.370	1.377	1.373	1.367	1.363
$rN_{22}C_9$	1.363	1.358	1.361	1.384		1.379	1.374	1.379	1.374	1.375	1.370
$rC_{11}N_{23}$	1.373	1.368	1.366	1.382		1.362	1.357	1.373	1.368	1.375	1.370
$rN_{23}C_{14}$	1.373	1.368	1.372	1.383		1.358	1.353	1.374	1.370	1.367	1.363
$rC_{16}N_{24}$	1.363	1.358	1.372	1.389		1.358	1.353	1.353	1.348	1.367	1.363
$rN_{24}C_{19}$	1.363	1.358	1.361	1.371		1.362	1.357	1.364	1.359	1.375	1.370
$\angle N_{21}C_4C_5$	125.6	125.6	125.7	124.8	(125.2)	128.6	128.6	127.3	127.3	129.8	129.8
$\angle C_4C_5C_6$	127.1	127.1	126.9	127.5	(127.1)	131.0	131.0	132.0	131.9	133.2	133.1
$\angle C_5C_6N_{22}$	125.5	125.6	125.5	125.1	(125.0)	128.6	128.6	131.1	131.0	129.8	129.8
$\angle C_6N_{22}C_9$	105.4	105.8	107.3	106.3	(106.1)	110.7	110.7	106.9	107.0	107.4	107.5
$\angle N_{22}C_9C_{10}$	125.5	125.6	125.4	125.6		123.2	123.3	121.4	121.5	120.7	120.9
$\angle C_9C_{10}C_{11}$	127.1	127.1	126.4	126.5		124.2	124.2	120.9	120.9	120.5	120.5
$\angle C_{10}C_{11}N_{23}$	125.6	125.6	125.5	125.0		123.0	123.1	120.9	121.1	120.7	120.9
$\angle C_{11}N_{23}C_{14}$	110.8	110.9	107.9	107.8	(108.6)	106.1	106.3	106.9	107.0	107.4	107.5
$\angle N_{23}C_{14}C_{15}$	125.6	125.6	125.9	125.1		127.0	127.1	130.9	130.9	129.8	129.8
$\angle C_{14}C_{15}C_{16}$	127.1	127.1	126.6	127.7		130.4	130.4	131.7	131.6	133.2	133.1
$\angle C_{15}C_{16}N_{24}$	125.5	125.6	125.4	124.1		127.0	127.1	126.0	126.0	129.8	129.8
$\angle C_{16}N_{24}C_{19}$	105.4	105.8	107.5	105.9		106.1	106.3	106.2	106.4	107.4	107.5
$\angle N_{24}C_{19}C_{20}$	125.5	125.6	125.1	125.3		123.0	123.1	122.7	122.9	120.7	120.9
$\angle C_{19}C_{20}C_1$	127.1	127.1	127.1	126.7		124.2	124.2	123.2	123.3	120.5	120.5
$\angle C_{20}C_1N_{21}$	125.6	125.6	125.7	125.8		123.2	123.3	122.7	122.8	120.7	120.9
$\angle C_1N_{21}C_4$	110.8	110.9	108.6	109.3		110.7	110.7	110.8	110.8	107.4	107.5

[a] A full set of optimized Cartesian coordinates is available from the authors on request
[b] Distances involving hydrogen cannot be determined accurately by X-ray crystallography

Fleischer [3]. Based on previous experience (e.g., see [27, 31, 32]) we consider an error of ≈0.02 Å in the computed TZ2P bond lengths between first-row atoms very unlikely. Crystal packing forces are also unlikely to change these bond lengths by such an amount. Although porphyrin has a fairly soft stretching vibrational mode, corresponding to the alternate expansion and contraction of the bonds along the conjugation path, the frequency of this mode is still above 700 cm^{-1} [14]. Our structure agrees qualitatively with a simple resonance model which predicts that the C_α—C_β distance is considerably shorter in the protonated than in the unprotonated pyrrole rings, while an opposite but somewhat smaller change is expected for the C_β—C_β and C_α—N bonds, with no change in the C_m—C_α bonds. The X-ray structure of Chen and Tulinsky [4] disagrees with this model. It appears that the position of the C_α atom is inaccurate in Ref. [4]. The large deviation from the theoretical predictions, the differences between the two X-ray investigations (the most recent of which was done

almost 25 years ago), and the disagreement with the (room temperature) NMR results all point to a need to reinvestigate the X-ray structure.

The calculated heavy-atom bond angles are in very good agreement with the averaged experimental values of Ref. [4]; apart from the $C_\alpha NC_\alpha$ angle (the CNC angle in the protonated pyrrole ring), which is 2.3° smaller than the theoretical value, the difference between theory and experiment is less than 0.6°. The major angle discrepancy again appears in a parameter connected with the position of C_α.

We do not compare calculated and experimental distances involving hydrogens, in view of the well-known inability of X-ray methods to locate hydrogen nuclei accurately. The inner hydrogen N—H distance quoted in Ref. [4], 0.86 Å, which has been used in some previous vibrational analyses, is certainly much too short [14].

Turning now to *cis*-porphyrin, we see (Table 1) that bond lengths between atoms in similar environments are similar to their corresponding values in *trans*-porphyrin – the basic structure of the pyrrole rings is essentially unaltered. The major changes, not surprisingly, are the distortions necessary to accommodate the repulsion between the inner *cis* imino hydrogens. The theoretical N—H bond length is 0.012 Å longer in *cis*-porphyrin than in *trans* and the $C_4N_{21}H_1$ angle is significantly larger (*cis*: 132°; *trans*: 124.6°). Additionally, there are changes in the linking CCC angles that connect the pyrrole rings: these angles (equal by symmetry) are around 127° in *trans*-porphyrin, but in the *cis* isomer they have widened to 131° in the imino-imino CCC link, to 130.4° in the link directly opposite, and contracted to 124.2° in the other two CCC links. Several of the NCC angles have also widened. These changes agree well with the geometrical differences between *cis*- and *trans*-porphyrin reported by Ghosh and Almlöf [22], although their actual calculated LDA parameters are somewhat different; in particular, the N—H bonds are too long at the LDA level (up to 1.06 Å in the *cis* isomer, a rather improbable value).

As expected from the Hammond postulate [33], the TS looks more like the *cis* than the *trans*-isomer. For instance, the distance involving the migrating inner-hydrogen atom in the TS (the N_{22}—H_2 distance) is around 1.29 Å, which is much closer to the 1.022 Å in *cis*-porphyrin than the 2.308 Å in the *trans* structure. There is considerable reorganization of the heavy atom skeleton during isomerization, e.g. the neighboring N...N distance, which is 2.927 Å in *trans*-porphyrin decreases to 2.502 Å in the transition state, and is 2.716 Å in the *cis* isomer. This reorganization has an implication for the tunneling rates.

Total energies for all four stationary points, with both the 6–31G(*d*) and TZ2P basis sets, are given in Table 2, along with relative energies, with and without zero-point vibrational energy (ZPVE) corrections. The latter were determined directly from the calculated 6-31G(d) harmonic vibrational frequencies. The ZPVE correction for the -d_2 isotopomer is also included.

The calculated DFT *cis*-*trans* energy difference is essentially the same with both basis sets, 8.4 and 8.3 kcal/mol; this also agrees closely with the MP2 value, 8.9 kcal/mol. The ZPVE correction changes the energy difference by only 0.2 kcal/mol. Our energy differences are slightly larger than those of Gosh and Almlöf [22] (7.0 and 7.6 kcal/mol without ZPVE correction at the LDA and MP2 levels, respectively). Experimental estimates of E_m, the minimum energy required for tunneling (which is probably an upper bound for the *cis*-*trans* energy difference), vary between 4.8–5.7 kcal/mol [21], the most recent result being 5.4_2 [19]. This is significantly lower than the calculated value. The origin of the discrepancy may be either imperfections in our calculations, or in the Bell [34] model used to deduce the barrier shape from experimental rate constants. Our best guess is that the calculated value is more reliable. There is no reason to expect significant differential correlation effects between the two tautomers. Our DFT energy difference is only slightly lower than the value obtained at the SCF level (11.1 kcal/mol with the 6-31G* basis, cf. 10.6 in Ref. [22]), and differs by only 0.5 kcal/mol from the MP2 result, showing that differential correlation effects are mild. A comparison of our two DFT calculations suggests that the results have converged with

Table 2. Absolute and relative energies (including ZPVE correction) for the four stationary points on the porphyrin PES relevant to the inner-hydrogen migration. (Absolute energies in hartrees, relative energies in kcal/mol; *trans*-porphyrin is taken as the energy zero)

Structure	Total energy	rel.	rel. + ZPVE(-*h*2)	rel. + ZPVE(-*d*2)
(a) B3-LYP/6-31G(*d*)				
trans	−989.530695	0.0	0.0	0.0
cis	−989.517309	8.4	8.2	8.2
TS	−989.503864	16.8	13.7	14.8
SS	−989.490188	25.4	19.3	21.2
(b) MP2/6-31G(*d*)//B3-LYP/6-31G(*d*)				
trans	−986.445138	0.0	0.0	0.0
cis	−986.430981	8.9	8.7	8.7
TS	−986.418020	17.0	13.9	15.0
SS	−986.405695	24.8	18.7	20.6
(c) B3-LYP/TZ2P				
trans	−989.891944	0.0	0.0	0.0
cis	−989.878680	8.3	8.1	8.1
TS	−989.866057	16.2	13.1	14.2
SS	−989.853123	24.4	18.3	20.2

respect to the basis set. Experimentally, the position of the *cis* minimum is determined mainly by the low-temperature kinetic data of Butenhoff and Moore [21]. These correlate well with the NMR data of Limbach and coworkers [18], indicating that this value is well determined within the modified Bell tunneling model. However, the model may have systematic errors. It would be of interest to carry out accurate dynamics calculations using our barrier data, augmented with a few points along the reaction path, and compare the results directly with experimental kinetics.

The *trans-cis* barrier of the -h_2 istopomer, including the significant (3.1 kcal/mol) ZPVE correction, is 13.7 kcal/mol at the B3-LYP/6–31G(*d*) level, diminishing to 13.1 kcal/mol with the TZ2P basis, and 13.9 kcal/mol at the MP2/6–31G(*d*) level. These values agree quite well with experimental estimates for the classical barrier height of 12–16 kcal/mol [21]. The most recent NMR study of Braun et al. [19], including for the first time tritium measurements, gives a value of 12.3 kcal/mol for the -h_2 isotopomer, while the previous best value was 12.9 kcal/mol [18]. In contrast to the *cis-trans* energy difference, the ZPVE correction is significant for the barrier height. The effective barrier is higher for D than for H migration. The calculated difference is 1.1 kcal/mol, which is near the upper limit of the experimental estimate of Butenhoff and Moore [21], 0.3–0.9 kcal/mol, but agrees well with the most recent value from Braun et al. [19], 1.2 kcal/mol. The reverse barrier, a measure of the stability of the *cis* isomer, is calculated to be only 5.0 kcal/mol.

The SS structure lies about 19 kcal/mol above the *trans* minimum (including ZPVE effects), which is more than 5 kcal/mol higher than the TS. It is a second-order saddle point, having two imaginary frequencies. Thus our calculations clearly predict that the inner-hydrogen migration occurs via a two-step mechanism involving the *cis* intermediate.

The single-point MP2/6-31G(*d*) relative energies calculated at the optimized B3-LYP/6-31G(*d*) geometries agree within 0.5 kcal/mol with the B3-LYP/6-31G(*d*) values, and within 0.8 kcal/mol with the B3-LYP/TZ2P results. In view of this excellent agreement between various methods, we believe that the predicted relative energies are accurate to about 1 kcal/mol, and are thus incompatible with a *cis-trans* energy difference of $\sim$5 kcal/mol.

The semiempirical AM1 [35] value for the *cis-trans* energy difference, 7.9 kcal/mol, agrees well with our calculations. However, the AM1 barrier heights are much higher: the *trans-cis* TS lies 37 kcal/mol above the *trans* minimum, with the SS structure lying a further 24 kcal/mol higher. The MP2 calculations of Reimers et al. [23] are only partially optimized and incorporate ZPVE corrections at the semiempirical PM3 level; they are thus not fully conclusive. They predict a barrier height of around 12 kcal/mol, in agreement with this work. We are, however, skeptical of their results for the SS structure. They obtain a (not fully optimized) MP2 barrier of 9 kcal/mol without ZPVE correction, which appears to be too low in the light of our results; most probably incomplete optimization is responsible. Their ZPVE correction for the SS state, calculated at the PM3 level, is 10 kcal/mol, which is much too large. These errors combine to predict an effective (ZPVE corrected) SS barrier which is *lower* than the *cis-trans* barrier, suggesting that the reaction is synchronous, in contradiction with most other theoretical and experimental predictions.

Can *cis*-porphyrin be detected experimentally? Braun et al. [18] estimated the tunneling lifetime of *cis*-porphyrin, extrapolated from low-temperature kinetic data to $1/T = 0$, to be only 10^{-8} s (note a misprint in their *A* value). This reasoning assumes that the tunneling state is close to the *cis* minimum, which is, however, not certain. A simple one-dimensional semiclassical (WKB) estimate [34] based on our imaginary frequency and cis energy, an inverted parabolic potential, and an effective mass of 2.5 amu gives an even lower lifetime estimate (10^{-9} s), in line with our low reverse barrier value. The effective mass was taken from the latest paper of Limbach and coworkers [19]. The value of 2.5 amu for H is not unreasonable in the light of our geometries, which show a substantial skeletal reorganization. Overall, it is very unlikely that *cis*-porphyrin-h_2 can be observed. The chances are somewhat higher of observing *cis*-porphyrin-d_2, and particularly the tritium isotopomer at low temperature, if the reverse barrier is significantly larger than our calculated value. It is also possible that asymmetric substitution in the ring may stabilize the *cis* isomer. The most promising route to *cis*-porphyrin appears to be the UV/visible [36] or infrared [37] photoexcitation of porphyrin-d_2 in cryogenic matrices.

As we have characterized each stationary point by a full vibrational analysis, we have a complete set of harmonic vibrational frequencies available for all four structures. These are useful for an RRKM analysis of the reaction rate at higher temperatures where tunneling effects are less significant, and perhaps for the identification of *cis*-porphyrin. The theoretical vibrational spectrum of *trans*-porphyrin has already been analyzed and excellent agreement obtained with experimental spectra using a scaled quantum mechanical (SQM) force field based on B3-LYP/6–31G* force constants [14, 15]. We have predicted the vibrational spectrum of *cis*-porphyrin using the same scale factors reported in Ref. [14] that were derived for *trans*-porphyrin. Our predicted transmittance spectra, reflecting the calculated IR intensities, for both *cis*- and *trans*-porphyrin-d_2 are shown in Fig. 3.

Looking at the scaled frequencies, there are two vibrational modes in *cis*-porphyrin-d_2 that have a large enough IR intensity and are sufficiently far from IR-active vibrations in *trans*-porphyrin to perhaps be used as "fingerprints" to detect the presence of the *cis* isomer. These are a predominantly C—H out-of-plane bend at 566 cm^{-1} (28 cm^{-1} away from the nearest IR-active mode in *trans*-porphyrin) and, especially, the N—D stretch at 2333 cm^{-1}, which is well removed from the corresponding trans mode at 2451 cm^{-1} (118 cm^{-1} lower). The N—D stretch is one of the most intense bands in the IR spectrum of *cis*-porphyrin-d_2 and the deuterium substitution effectively isolates this band from the other modes. The problem is, of course, that any signals from *cis*-porphyrin are likely to be almost completely swamped by signals from the much greater concentration of the *trans* isomer. The third spectrum in Fig. 3 is a

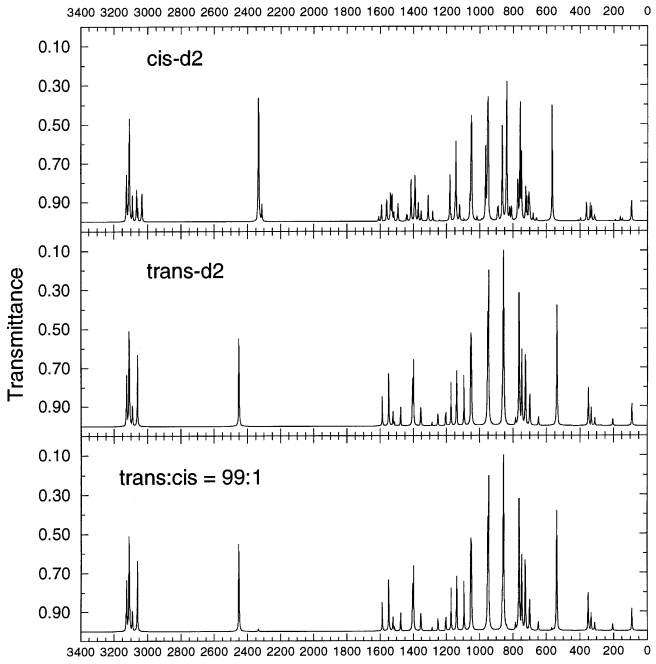

Fig. 3a–c. Calculated IR vibrational spectrum (transmittance) for: **a** *cis*-porphyrin-d_2; **b** *trans*-porphyrin-d_2; **c** a mixture of 99% *trans* and 1% *cis*. (The small peak at 2333 cm^{-1} in the mixed spectrum is due to the *cis* isomer)

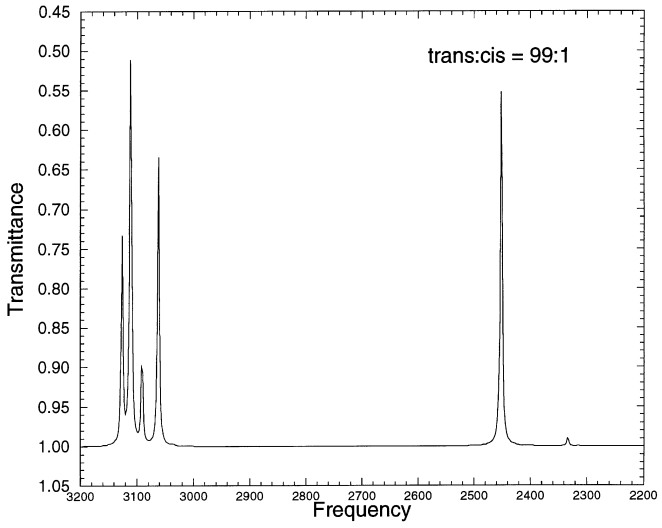

Fig. 4. Calculated IR vibrational spectrum (transmittance) in the 2200–3200 cm^{-1} region for the 99% *trans*/1% *cis* mixture on an expanded scale showing the 2333 cm^{-1} *cis* "fingerprint"

mixed *trans-cis* spectrum assuming only 1% of the *cis* form, the other 99% being *trans*-porphyrin-d_2. The intense signal at 2333 cm^{-1} in the *cis* spectrum can be seen as a very small peak in the mixed *trans-cis* spectrum; however it *may* be detectable provided a sufficiently "clean" and well-resolved spectrum could be taken. Figure 4 shows the region from 2200–3200 cm^{-1} on an expanded scale; the small peak at 2333 cm^{-1} is the *cis* "fingerprint".

We have calculated rate constants for the *trans* $\longrightarrow$ *cis* isomerization using transition state theory in the rigid rotor-harmonic oscillator approximation. In this theory, the unimolecular reaction rate is give by the equation

$$k^L = \kappa\ (kT/h)[Q(TS)/Q(\text{trans})]\exp[-E/RT] \qquad (1)$$

where $Q(TS)$ is the total partition function for the transition state and Q(trans) that for *trans*-porphyrin (with $Q = q_{\text{translation}}q_{\text{rotation}}q_{\text{vibration}}$), and E is the barrier height (including ZPVE effects). L is a hydron (H, D or T), and κ is the transmission coefficient, which was assumed to be 1.0 . Calculated rate constants (using our scaled frequencies) at various temperatures are displayed in Table 3, along with experimental values of Limbach and coworkers [18, 19]. For consistency reasons, we have compared our data to the fitted values of Braun et al. [19], as defined in their footnote (9) [38], and not to the direct experimental measurements. The difference of the two seldom exceeds 20% and thus the fit is accurate by the standards of rate constant determination.

The *trans* $\longrightarrow$ *cis* reaction path is fourfold degenerate. This factor is normally included in the symmetry number of the rotational partition functions in Eq. (1) and does not have to be taken into account separately [39]. However, to be compatible with the rate constant values quoted by Braun et al. [19], the rate constant corresponding to the migration of a single hydron is given in Table 3, i.e., we use a symmetry number of two.

As expected, our calculated values, which neglect tunneling, are lower than the experimental ones, particularly for H transfer and at low temperatures. The agreement improves as the mass of the hydron and the temperature increases, showing that the bulk of the discrepancy is due to tunneling. As expected, the observed kinetic isotope effects (at 298 K, $k^H/k^D \approx 11.3$, $k^D/k^T \approx 3.4$, see Ref. [19]; these values are in rough agreement with those observed by Butenhoff and Moore [21] in hexane matrices) are also much larger than our values calculated without tunneling, (4.6 and 2.0, respectively). The calculated ratio $\ln(k^H/k^T)/\ln(k^H/k^D)$ is 1.45, close to the Swain-Schaad ratio of 1.442 for nontunneling barrier reactions [40].

Table 3. Rate constants (s^{-1}) for the hydrogen migration in *trans*-porphyrin. Calculated values using Eq. (1) (this work); experimental values from the Arrhenius fits of Braun et al. [19]

T/K	log k^H_{calc}	log k^H_{expt}	log k^D_{calc}	log k^D_{expt}	log k^T_{calc}	log k^T_{expt}
319	3.60	4.63	2.98	3.70	2.69	3.21
309	3.30	4.43	2.66	3.44	2.37	2.93
304	3.14	4.33	2.49	3.31	2.19	2.79
298	2.95	4.20	2.28	3.14	1.98	2.61
290	2.67	4.02	1.99	2.90	1.68	2.36
280	2.30	3.78	1.60	2.59	1.29	2.03
270	1.91	3.52	1.19	2.26	0.88	1.68
260	1.48	3.25	0.74	1.90	0.40	1.29

4 Conclusions

We have carried out the most comprehensive calculations on the *trans-trans* inner-hydrogen migration in free base porphyrin performed to date. Our best results are based on fully optimized structures obtained at the B3-LYP/TZ2P level (726 basis functions) incorporating ZPVE effects calculated using analytical frequencies obtained with the 6–31G(*d*) basis. These results have been confirmed by single point MP2 energy calculations at the stationary points. Although our TZ2P geometry for *trans*-porphyrin agrees reasonably well with the D_{2h} averaged X-ray structure of Chen and Tulinsky [4], it appears that the position of the C_α atom in their structure is in error by about 0.02 Å. The calculations show conclusively that the hydrogen migration occurs via a two-step mechanism involving a metastable *cis* intermediate, in agreement with experimental kinetic isotope effect data [18]. Our best value for the *trans-cis* barrier height is 13.1 kcal/mol, and for the *trans-cis* energy difference is 8.1 kcal/mol in the -h_2 istopomer. The former value is in good agreement with the experimental data derived from modeling the tunneling [18, 19], but the latter is higher than the experimental estimates. In view of the insensitivity of the *cis-trans* energy difference to correlation and basis set effects, and the good agreement between the density functional and MP2 results, we believe that the calculated data are more accurate. There is substantial skeletal reorganization during the hydron shift. The *trans-cis* reaction rates calculated from transition state theory are too low by factors ranging from nearly 60 at low temperature (260 K) for H migration to less than 3 for T migration at 319 K, showing the importance of tunneling.

From a vibrational analysis of *cis*-porphyrin-d_2 we propose that the IR active N—D stretching mode at 2333 cm^{-1} might serve as a fingerprint to detect the *cis* isomer in the presence of the more stable *trans* form. Assuming a "clean" spectrum, this signal is predicted to be sufficiently intense and far enough removed from nearby *trans* signals to be detectable in mixtures containing only 1% of the *cis* form.

Acknowledgements. We thank Dr. Marek Zgierski (NRC, Canada) for performing the frequency calculation on our optimized TS structure (which was stretching our computational resources), and Prof. H.-H. Limbach (Berlin) for valuable comments and preprints. This work was supported by the Air Force Office of Scientific Research under grant no. F49620-94-1-0072 and the National Science Foundation under grant no. CHE-9319929.

References

1. Fischer H, Orth H (1937) Die Chemie des Pyrrols, vol. II, part 1. Akademic Verlag, Leipzig
2. Dolphin D (ed) (1978) The porphyrins, Academic Press, New York
3. Webb LE, Fleischer EB (1965) J Chem Phys 43:3100
4. Chen BML, Tulinsky A (1972) J Am Chem Soc 94:4144
5. Frydman L, Olivieri AC, Diaz LE, Frydman B, Morin FG, Mayne CL, Grant DM, Adler AD (1988) J Am Chem Soc 110:336
6. Radziszewski JG, Nepras M, Balaji V, Waluk J, Vogel E, Michl J (1995) J Phys Chem 99:14254
7. Almlöf JE (1974) Int J Quantum Chem. 9:8
8. Rawlings DC, Davidson ER, Gouterman M (1982) Theor Chim Acta 61:227
9. Reynolds CH (1988) J Org Chem 53:6061
10. Foresman JB, Head-Gordon M, Pople JA, Frisch MJ (1992) J Phys Chem 96:135
11. Almlöf JE, Fischer TH, Gassman PG, Ghosh A, Häser M (1993) J Phys Chem 97:10964
12. Merchan M, Orti E, Roos BO (1994) Chem Phys Lett 221:136
13. Kozlowski PM, Zgierski MZ, Pulay P (1995) Chem Phys Lett 247:379
14. Kozlowski PM, Jarzecki AA, Pulay P (1996) J Phys Chem 100:7007
15. Kozlowski PM, Jarzecki AA, Pulay P, Li XY, Zgierski MZ (1996) J Phys Chem 100:13985
16. Storm CB, Teklu Y, (1972) J Am Chem Soc 94:1745
17. Wehrle B, Limbach H-H, Köcher M, Ermer O, Vogel E (1987) Angew Chem Int Ed Engl 26:934
18. Braun J, Schlabach M, Wehrle B, Köcher M, Vogel E, Limbach H-H (1994) J Am Chem Soc 116:6593 and references therein
19. Braun J, Limbach H-H, Williams PG, Morimoto H, Wemmer DE (1996) J Am Chem Soc 118:7231
20. Eaton SS, Eaton GR (1977) J Am Chem Soc 99:1601 (note that this paper deals not with the parent porphyrin but with tetraaryl porphyrins, although it is unlikely that the mechanisms differ)
21. Butenhoff TJ, Moore CB (1988) J Am Chem Soc 110:8336
22. Ghosh A, Almlöf JE (1995) J Phys Chem 99:1073
23. Reimers JR, Lü TX, Crossley MJ, Hush NS (1995) J Am Chem Soc 117:2855
24. Becke AD (1993) J Chem Phys 98:5648
25. Lee C, Yang W, Parr RG (1988) Phys Rev B 41:785
26. Frisch MJ, Trucks GW, Schlegel HB, Gill PMW, Johnson BG, Robb MA, Cheeseman JR, Keith T, Petersson GA, Montgomery JA, Raghavachari K, Al-Laham MA, Zakrzewski VG, Ortiz JV, Foresman JB, Cioslowski J, Stefanov BB, Nanayakkara A, Challacombe M, Peng CY, Ayala PY, Chen W, Wong MW, Andres JL, Replogle ES, Gomperts R, Martin RL, Fox DJ, Binkley JS, Defrees DJ, Baker J, Stewart JJP, Head-Gordon M, Gonzales C, Pople JA (1995) GAUSSIAN 94, revision C.3. Gaussian, Inc., Pittsburgh, PA
27. Baker J, Muir M, Andzelm J, Scheiner A (1996) In: Laird BV, Zeigler T, Ross R, (eds) Chemical applications of density functional theory. pp 342–367 American Chemical Society, and references therein
28. Baker J, Muir M, Andzelm J (1995) J Chem Phys 102:2063
29. Wiest O, Black KA, Houk KN (1994) J Am Chem Soc 116:10336
30. Schafer A, Horn H, Ahlrichs R (1992) J Chem Phys 97:2571
31. Muir M, Baker J (1996) Mol Phys 89:211
32. Munakata H, Kakumoto T, Baker J (1997) J Mol Struct (Theochem) 391:231
33. Hammond GS (1955) J Am Chem Soc 77:334
34 Bell RP (1980) The tunnel effect in chemistry. Chapman and Hall, London
35. Smedarchina Z, Siebrand W, Zerbetto F (1989) Chem Phys 136:285
36. Völker S, van der Waals JH (1976) Mol Phys 32:1703
37. Butenhoff T, Chuck RS, Limbach HH, Moore CB (1990) J Phys Chem 94:7847
38. Note that the Arrhenius equation for tritium transfer in footnote (9) of Ref. [19] is incorrect. The correct equation is $k^T = 10^{11.64}\exp(-51.5\ kJ\ mol^{-1}/RT)$, given in the supplementary material
39. Forst W (1973) Theory of unimolecular reactions. Academic Press, New York, p 91
40. Swain CG, Stivers EC, Reuwer JF, Schaad LJ (1958) J Am Chem Soc 80:5885